



HAL
open science

Drug Target Engagement using coupled Cellular Thermal Shift Assay -acoustic Reverse Phase Protein Array

Adrien Herledan, Marine Andres, Aurore Lejeune-Dodge, Florence Leroux, Alexandre Biela, Catherine Piveteau, Sandrine Warengem, Cyril Couturier, Benoit Deprez, Rébecca F. Déprez-Poulain

► **To cite this version:**

Adrien Herledan, Marine Andres, Aurore Lejeune-Dodge, Florence Leroux, Alexandre Biela, et al.. Drug Target Engagement using coupled Cellular Thermal Shift Assay -acoustic Reverse Phase Protein Array. *Slas Discovery*, 2019, 25 (2), pp.207-214. 10.1177/2472555219897256 . hal-03051837

HAL Id: hal-03051837

<https://hal.science/hal-03051837>

Submitted on 10 Dec 2020

HAL is a multi-disciplinary open access archive for the deposit and dissemination of scientific research documents, whether they are published or not. The documents may come from teaching and research institutions in France or abroad, or from public or private research centers.

L'archive ouverte pluridisciplinaire **HAL**, est destinée au dépôt et à la diffusion de documents scientifiques de niveau recherche, publiés ou non, émanant des établissements d'enseignement et de recherche français ou étrangers, des laboratoires publics ou privés.

Drug Target Engagement using coupled Cellular Thermal Shift Assay - acoustic Reverse Phase Protein Array

Adrien Herledan ^a, Marine Andres ^{a,c}, Aurore Lejeune-Dodge ^b, Florence Leroux ^{a,c},
Alexandre Biela ^a, Catherine Piveteau ^a, Sandrine Warenghem ^a, Cyril Couturier ^a, Benoit
Deprez ^{a,c}, Rebecca Deprez-Poulain ^{a,c,d}

^a *Univ. Lille, Inserm, Institut Pasteur de Lille, U1177 - Drugs and Molecules for Living Systems, F-59000 Lille, France*

^b *LABCYTE INC, 170 Rose Orchard Way, San Jose, CA 95134, USA*

^c *European Genomic Institute for Diabetes, EGID, University of Lille, F-59000, France.*

^d *Institut Universitaire de France (IUF), 75231 Paris, France*

Corresponding author: Tel: +33 (0)3 20 87 71 36.

E-mail address: adrien.herledan@inserm.fr.

Keywords: Target Engagement, CETSA, RPPA, Acoustic transfer, Drug Discovery, Nanovolume, Insulin-Degrading Enzyme

Abstract

In the last five years, Cellular Thermal Shift Assay, a technology based on ligand-induced changes in protein thermal stability, has been increasingly used in drug discovery to address the fundamental question of whether drug candidates engage their intended target in a biologically relevant setting. To analyze lysates from cells submitted to increasing temperature, the detection and quantification of the remaining soluble protein can be achieved using quantitative mass spectrometry, Western blotting or AlphaScreen® techniques. Still, these approaches can be time- and cell-consuming. To cope with limitations of throughput and protein amount requirements, we developed a new coupled assay combining the advantages of nano-acoustic transfer system and reverse phase protein array technology within CETSA experiments. We validated the technology to assess engagement of inhibitors of Insulin Degrading Enzyme (IDE), an enzyme involved in diabetes and Alzheimer's disease. CETSA - acoustic Reverse Phase Protein Array (CETSA-aRPPA) allows simultaneous analysis of many conditions and drug-target engagement with small sample size, and in a rapid, cost-effective and biological material-saving manner.

Introduction

In the past few years, Cellular Thermal Shift Assay (CETSA) has emerged as an essential tool to explore target engagement and target validation in drug discovery, directly in the complex environment of intact cells.¹ It is increasingly used also to guide medicinal chemistry efforts and lead optimization.^{2,3} CETSA is based on the ligand-induced stabilization of the targeted protein (**Fig.1A**).² After lysis of cell samples previously incubated in the presence or absence of ligand and subsequently heated at various temperatures, aggregation protein profile is determined by measuring folded protein remaining in the cell lysate. The alteration of heat-induced aggregation by a small molecule binding to the protein, causes a shift (also referred to as thermal shift) in the aggregation temperature (Tagg). Along with the increasing use of CETSA, various detection methods have been developed,² either based on homogeneous detection,^{4,5} high-resolution mass spectrometry,^{6,7} or image analysis^{8,9} (**Fig.1A**).

To support decision making and compound selection in drug discovery, it is critical that the tools allows to test numerous compounds and thus the throughput of CETSA needs to be increased. In this context, CETSA has been successfully coupled with AlphaLISA® detection to screen androgen receptors ligands and to determine the agonist or antagonist binding mode of compounds.¹⁰ Alternatively, enzyme fragment complementation (EFC), that are based on protein modification with a tag, allows detection of non-aggregated protein by addition of the enzyme acceptor (EA) fragment, in a high throughput manner. This technique has been applied for the discovery of SMYD3 inhibitors using β -galactosidase-derived fragment, or for the screening of CDK9 inhibitors using a fragment of NanoLuc (NLuc).^{11,12} These latest developments

have greatly improved throughput but require nonetheless specific assay development. Indeed, CETSA AlphaLISA® requires the availability and optimization of a pair of antibodies. As well, CETSA EFC requires the production of the tagged–target and the checking of the absence of alteration of T_{Agg} of fused protein-tag compared to untagged protein. Also, it is based on the production of a tagged protein within cell which expression can dramatically differ from that of the native protein.

As a result, Western blot (WB) is still the most used readout to quantify folded protein target in CETSA protocols. However, this method leads to a large amount of data points to analyse, requires substantial cell amounts and is labour intensive when many compounds or parameters have to be tested. In this context, we propose to couple Reverse Phase Protein Array (RPPA) technology to CETSA (**Fig.1B**). RPPA can be fully adapted to measure protein target signal at high throughput with minimal sample consumption. Thanks to the use of highly specific primary antibodies and automation allowing printing of replicates, the technique is both robust and quantitative. Also, we use the most recent developments in the field of the Acoustic Droplet Ejection Technology¹³ for microarraying. To validate this method, we explored target engagement of inhibitors of Insulin Degrading Enzyme (IDE). CETSA-aRPPA successfully provided insights into compound profiles and IDE target engagement in hepatocytes.

Material and Methods

Cell culture and compound treatments

HepG2 cells provided by Dr. Nathalie Hennuyer (Institut Pasteur de Lille, France) were cultured in gelatin (Sigma-Aldrich, G-1890, 1 mg/mL) pre-coated T75 flasks in MEM Alpha Medium (1X) + GlutaMax (Gibco, 32561-029) containing 10% heat-inactivated

fetal calf serum (Life Technologies, 10270-106) and 5 µg/mL penicillin/streptomycin (Life Technologies, 15070-063), in 37 °C humidified incubator with 5% CO₂ atmosphere. After the cells had grown to confluence, vehicle or compounds (**1-2** in-house compounds, **3** (6bK)) were added to 30 µM final concentration (0.3% final DMSO).

CETSA

Suspended HepG2 cells were washed in PBS and detached using trypsin/EDTA solution (Life Technologies, 25300054). Cells were transferred in medium in 15 mL falcon and centrifuged at 300 g during 4 min. Supernatant was then discarded and cells were washed in PBS (Gibco, DPBS (1X), 14190-094), counted and centrifuged at 300g during 4 min. After removing PBS, cells were suspended in Tris Buffered Saline 1X (TBS 10X, Euromedex, ET220-B) at the 10 million per mL and aliquoted in 10 PCR 0.2 mL microtubes (Thermo Scientific, AB-0622) for each condition with 50 µL. Tubes were then transiently heated to a range of temperature from 40 °C to 67 °C for 3 min using a SureCycler 8800 Thermal Cycler (Agilent Technologies), cooled at room temperature for 3 minutes and followed by three freeze/thaw cycles in liquid nitrogen. Insoluble proteins were separated by centrifugation (20000 g, 20 min, 4 °C) and 35 µL of supernatant corresponding to soluble proteins were kept for Western blot or Reverse Phase Protein Array analysis. Three independent experiments were performed for each compound. For ITDRF_{CETSA-aRPPA} see Supplementary Methods.

SDS PAGE Electrophoresis with CETSA samples

Each total protein sample (7 µL) were prepared and heated at 70 °C for 10 min with NuPAGE™ Sample Reducing Agent (10X) (ThermoFischer Scientific, NP0004) and

NuPAGE™ LDS Sample Buffer (4X) (ThermoFisher Scientific, NP0007), loaded in NuPage 3-8% Polyacrylamide gel for migration (150V, 1 hour) and then transferred on nitrocellulose membrane (Amersham Protran supported 0.2 µm NC, 10600080) with iBlot™ 2 Gel Transfer Device (ThermoFisher Scientific, IB21001).

Immobilization of CETSA samples and purified IDE on nitrocellulose by nanoacoustic transfer

Labcyte 384 LDV microplate (LP-0200) was loaded with CETSA protein samples and TBS BSA 1% solution with 50 and 100 ng/mL of IDE as controls, left at RT for 2 hours to perform the protein saturation of microplate plastic (Cyclic olefin copolymer) and centrifuged without seal at 1500 g for 2 min with medium deceleration velocity. Using acoustic liquid handling device (Labcyte, Echo 550) and Echo array Maker software, 20 nL lysate or protein sample was transferred on nitrocellulose membrane (Amersham Protran supported 0.2 µm NC, 10600080) fixed on a glass slide maintained on a slide holder (Tecan, 30065759). After 2 hours at RT, membranes were stored at 4 °C until final disposal.

Immunoblotting for WB and RPPA

Blots and printed membranes were blocked in dry milk (5%) diluted in PBS for 1 hour at RT and washed 3 times of 10 min in PBS 0,1% Tween 20. Mouse monoclonal anti-IDE antibody (Santa Cruz Biotechnology, clone F-9, sc-393887) were used as primary antibody diluted at 1:1000 for WB or 1:2500 for RPPA in 2% BSA PBS 0,1% Tween20 solution and incubated respectively 1h30 for WB and 30 min for RPPA at RT. After 3 washes in 0.1% PBS Tween 20, Anti-Mouse IRDye 800 CW (Licor IRDye 800CW Goat anti-Mouse IgG, P/N 925-32210) was used as secondary antibody in 2% BSA PBS

0,1% Tween 20 solution at 1:20000 for 1h30 at RT and blots were washed 3 times in PBS Tween 0,1% before fluorescence intensities detection by Odyssey CLx Imaging System.

Data analysis and aggregation curve

The signal intensities (corresponding to sample fluorescence minus background fluorescence) of each protein band or spot on the Western blots or Reverse Phase Protein Arrays were quantified using Image Studio™ Lite Analysis Software (Licor). Fold-changes were calculated in percentage of the lowest temperature. The relative signals were plotted against temperature using Graphpad (Prism) and a variable slope sigmoidal curve was fitted using the chemical denaturation theory equation.

$$f(T) = \left(\frac{1 - plateau}{1 + e^{-\left(\frac{a}{T} - b\right)}} \right) + plateau$$

Initial values for top and bottom plateau were set at 100% and 0% respectively for curve fitting. Aggregation curves were expressed independently for each experiment or as means of multiple experiments (n = 3) +/- SEM. Thermal shifts were calculated using ΔT_{Agg50} , as the difference in aggregation temperatures between the control and treatment, at which 50% signal intensity (protein denaturation) was observed.

Determination of IDE inhibition by compounds

Recombinant human IDE (IDE) was provided by Pr W.J. Tang (University of Chicago). The enzymatic activity of IDE was assayed quantifying the amount of insulin (Actrapid®, Novo Nordisk) at the end of the incubation period. 19.6 μ L of *wt* IDE in HEPES buffer (50 mM with 100 mM NaCl, pH 7.4) at 300 ng/mL were pre-incubated 15

minutes at room temperature with 400 nL of test compound or vehicle (DMSO) transferred with Echo 550 in 96 well half-area microplate (Corning, 3686). The reaction was then started by the addition of 20 μ L of insulin at 40 nM. The final concentration of IDE and substrate was 0.25 μ g/mL and 20 nM, respectively. Incubations were performed at ambient temperature for 10 minutes. The reaction was then stopped by addition of 40 μ L of 200 mM EDTA. The samples were diluted by 10 in AlphaLISA® diluant. 2 μ L of samples or standard were incubated with 8 μ L of a 2.5X mix of AlphaLISA® Anti-insulin Acceptor beads, biotinylated antibody Anti-insulin and AlphaLISA® immunoassay Buffer in 384 well Proxiplate (Perkin Elmer, AL204C). The microplate was sealed and left on the bench for 60 min at room temperature. 10 μ L of a mix SA-Donor beads and AlphaLISA® immunoassay Buffer were added and the plate was read with Mithras LB 940 reader (Berthold) with Alphascreen® protocol at 620 nm after 30 min of incubation. IC₅₀ values were calculated using XLfit 5 software from concentration-response curves fitted by a nonlinear regression analysis to the 4 parameter logistic equation:

$$y = A + \frac{B - A}{1 + \left(\frac{10^C}{x} \right)^D}$$

A, minimum y value; B, maximum y value; C, LogIC₅₀ value; D, slope factor.

Results and Discussion

Insulin-Degrading Enzyme (IDE) is a ubiquitous protease involved in the degradation of many peptides, like insulin, that share a propensity to be amyloidogenic. IDE has an atypical structure that is able to undergo a large conformational shift from full closed to fully open states. CryoEM studies on IDE revealed recently how amyloidogenic peptides are captured and hydrolyzed by IDE.¹⁴ In the recent years,

several exosite-binding inhibitors BDM43124¹⁵⁻¹⁶ or **3** (6bK) a macrocyclic peptide,¹⁷ or drug-like catalytic-binding **1** (BDM44768) discovered by *in situ* click chemistry strategy¹⁸ were disclosed. Surprisingly, **1** (BDM44768) and **3** (6bK) display different effects on glucose tolerance *in vivo*, suggesting the complex role of IDE in this phenotype. As well, Villa-Perez et al recently revisited, using liver-specific IDE *ko* mice, the role of IDE in hepatic insulin resistance.¹⁹ Wishing to contribute to the understanding of the role of IDE in hepatocytes, we wanted to select the best chemical tool among published inhibitors. We thus turned ourselves to CETSA technique to select a compound that actually engages IDE in hepatocytes.

Design and validation of CETSA-aRPPA

In the described assay, we propose to analyze the soluble protein fraction obtained from CETSA experiments by RPPA approaches consisting in immobilization of samples on a nitrocellulose support and subsequent detection by immunoblotting with an antibody directed against the protein of interest. HepG2 cells have been treated during 2 hours with compounds **1-3** (30 μ M) or DMSO. Cells were then heated at 10 different temperatures between 40 °C and 67 °C. Soluble protein lysates corresponding to each condition of treatment were printed on nitrocellulose membrane using acoustic nanodispensing (see below). RPPA pattern used purified IDE recombinant protein (50 ng/mL and 100 ng/mL) as positive control and buffer alone for negative control. Three independent biological replicates have been carried out using an RPPA pattern (**Suppl. Fig. S1**). A first series of experiments allowed us to measure the linearity of IDE detection using acoustic transfer and RPPA. Then of our CETSA-aRPPA tool versus WB comparing the aggregation curves and the determined aggregation temperature corresponding to 1-3 compounds. Furthermore, these

CETSA protein extracts samples have been used to evaluate the precision of CETSA-aRPPA for three independent microarray patterns as well as permeability of compounds.

Linearity of IDE detection using acoustic transfer and RPPA technologies

Immobilization of protein samples or purified IDE on the array was set up using Echo acoustic liquid handling technology.²⁰ Lysates were transferred by using sound energy achieved by transducer from source well of 384 low-dead-volume microplate to nitrocellulose membrane, and which provide contact-less fluid dispensing. This destination support is fixed on a glass slide, held in a specific handler which is inverted in order to place the membrane above the source well (**Suppl. Fig. S2**). Spots of protein samples correspond to 20 nL transfer (8 droplets of 2.5 nL). To validate the correlation between IDE signal detected by fluorescence and concentration of this protein target, we have printed 20 nL of IDE protein from 50 µg/mL to 2.5 ng/mL. Pictures acquired after immunoblotting development corresponding to 3 drop-off of IDE range (10 concentrations) are shown in **Suppl. Fig. S3**. A very good linear correlation ($r^2 = 0.9695$) between IDE concentration and fluorescence signal was measured.

Accuracy and precision of RPPA versus WB

In order to avoid the detection of unrelated proteins in RPPA approach, the high specificity of antibody directed against IDE (110 kDa) has been checked in WB on HepG2 protein extracts. The second strongest band (90 kDa) was found to have an intensity below 5% of the specific signal at 110 kDa, qualifying the antibody RPPA quantification. (**Suppl. Fig. S4**). Quantified signals obtained from CETSA experiments (in WB and CETSA-aRPPA) were normalized for each condition of treatment with the

signal at the lowest temperature (40 °C) corresponding to 100% of non-aggregated protein. Using the chemical denaturation theory formula, the data were fitted to obtain an aggregation curve of IDE in presence or in absence of inhibitors. To evaluate the accuracy of the CETSA-aRPPA *versus* Western Blot, three biological experiments for each method underwent the same analysis process (**Fig. 2A** and **2B** respectively, **Suppl. Fig S5-6**). Fitted aggregation curves on the three series allowed to determine T_{Agg} values corresponding of the temperature at 50% of aggregated IDE and ΔT_{Agg} for each condition. For DMSO and the tested inhibitors **1-3**, both methods gave consistent results (**Fig. 2A** and **2B** and **Suppl. Table S1**). Indeed, the T_{Agg} determined by WB or CETSA-aRPPA for each condition of treatment have been compared with one way ANOVA statistic test (**Fig. 2C**). No significant difference between methods could be established for DMSO or inhibitors **1-3** and this resulted in a good correlation ($r^2 = 0.9951$ **Fig. 2D**). Spotting precision of CETSA-aRPPA has been studied by comparing T_{Agg} calculated in three assay replications (P1: Pattern1, P2: Pattern2, P3: Pattern3) as the mean of three T_{Agg} corresponding to each experiment. Images of these three patterns have been analyzed and signals corresponding to IDE have been quantified in order to fit aggregation curves and calculate T_{Agg} (see **Fig. 2E** and **Suppl. Fig. S4**). No significant difference between T_{Agg} obtained into each condition of treatment has been observed when we compared the three patterns.

Cellular target engagement of IDE by inhibitors

The three compounds (**Fig. 3A**) with inhibitory activities on IDE (enzymatic assay) in the same range ($6.5 < pIC_{50} < 6.9$, **Fig. 3B**) were selected to study target engagement of IDE in hepatocytes. Compounds **1** (BDM44768) and **2** derive from a series of triazoles targeting the catalytic site of IDE and were discovered by *in situ* click

chemistry, (**Fig. 3A-B**).¹⁸ Inhibitor **3** (6bK) is a macrocycle discovered by DNA-templated library, and targets an exosite (**Fig. 3A-B**).¹⁷ Aggregation profile of IDE in the presence of inhibitors **1-2** showed a significant shift (**Fig. 2B and 3C**). Interestingly bis-fluorinated analog **2** stabilizes IDE better than **1** ($\Delta T_{\text{Agg}} = 5.63 \text{ }^{\circ}\text{C}$ vs $3.06 \text{ }^{\circ}\text{C}$ respectively). On the contrary, treatment of cells with **3** did not achieve significant stabilization of IDE versus control ($\Delta T_{\text{Agg}} = -0.36 \text{ }^{\circ}\text{C}$).

Using the same CETSA-aRPPA technique we measured the dose-dependent IDE stabilization (ITDRF: isothermal dose–response fingerprint) by compound **1** (**Fig. 4A, Suppl. Fig. S7, Suppl. methods**) and **2** (**Fig. 4B**). To rationalize CETSA-aRPPA and ITDRF_{CETSA-aRPPA} results, we measured the ability of inhibitors **1-3** to cross the membrane of HepG2 cells (**Fig. 4C Suppl. Table S2 and Suppl. methods**). Compounds were titrated by LC-MS/MS in cell culture medium and in HepG2 cells using samples from the CETSA experiments. Permeability was expressed as the ratio of concentrations of inhibitors in cells *versus* in the extracellular medium at the end of the diffusion period (2 hours). While inhibitors **1** and **2** penetrate HepG2 cells, inhibitor **3** was not detected in HepG2. So, the poor result of **3** in CETSA can be attributed to its poor permeability. Interestingly, while inhibitors **1** and **2** display similar inhibitory potencies on IDE (IC_{50}), **2** engages IDE in cells 10 times more efficiently than **1** (EC_{50} of $2.75 \text{ } \mu\text{M}$ vs $25.5 \text{ } \mu\text{M}$ respectively) (**Fig. 4D**). Like **1**, compound **2** chelates zinc ion with its hydroxamic acid, makes a cation- π interaction with Arg824 *via* the triazole ring and a hydrogen bond with Ser138 *via* the carbonyl of the amide bond (**Fig. 4E**). The introduction of the second fluorine in compound **2** enhances IDE inhibition by allowing phenyl ring to better engage π -stacking with Phe820, and by engaging naphthyle in an interaction with the backbone of Val833 (**Fig. 4E, Suppl. Fig. S8, Suppl. methods**). Introduction of the fluorine increases interactions with the target, decreases the

aqueous solubility and desolvation energy and enhances LogD by 0.4 (**Fig. 4D, Suppl. methods**). This explains the high potency and better permeability of this compound, translating into a higher ΔT_{Agg} .

Interestingly, potency shift between acellular inhibitory assay (IC_{50}) and cellular engagement assay (EC_{50}) is 3 times lower for compound **2** (21) than for compound **1** (77). As the relative permeability of compounds **1** and **2** differs also by a factor of 3, the potency shift varies mainly in function of the relative permeability of the two compounds.

ITDRF is more relevant to measure target engagement in cells than measuring the global intracellular concentrations of compounds because these could have an uneven cellular distribution. For our chemical series however the potency shift seems to be correlated to the ability to penetrate HepG2 cells.

Compound **2** is thus the best candidate to explore the role(s) of IDE in hepatocytes, while *in vivo* effects of **3** (6bK) may be only attributed to inhibition of extracellular IDE, a small fraction of IDE in the body.

Target engagement in whole cells or tissues has become a fundamental step in drug discovery projects in order to select drugs candidates before preclinical studies or to confirm functional effects of chemical compounds. In this context, CETSA is a tool of choice to study target engagement. This approach considers addressing, permeability and general protein-binding aspects and permits direct measurement of ligand binding to target protein. Nevertheless, despite an easy implementation for the most laboratories, application to large chemical series or libraries remains challenging. Based on new features of nanoacoustic transfer device, we developed CETSA-aRPPA

technology with the objective to propose a new valuable tool to explore target engagement with a higher-throughput than conventional and actual analysis techniques and a lower consumption of samples. The method displays a high precision and accuracy compared to Western Blot. It was used to study target engagement of IDE by inhibitors in whole HepG2 cells context. aRPPA detection can also be used to measure ITDRF dose-dependent stabilization of target of interest (ITDRF_{CETSA-aRPPA}) with the same advantages. In the future CETSA-aRPPA will allow further applications including screening or multitarget engagement studies.

Acknowledgments

The authors would like to thank Dr. Nathalie Hennuyer for the kind gift of HepG2 cell line and Pr Wei-Jen Tang for human recombinant IDE.

Declaration of Conflicting Interests

The authors declared no potential conflicts of interest with respect to the research, authorship, and/or publication of this article.

Funding

The authors acknowledge financial support from INSERM, University of Lille, Institut Pasteur de Lille, Region Nord Pas de Calais, FEDER, State (0823007, 0823008, 07-CPER 009-01, 2007-0172-02-CPER/3), the European Union under the European Regional Fund (ERDF), by the Hauts-de-France Regional Council (contract N°17003781), the MEL (contract N°2016_ESR_05), and the French State (contract N°2017-R3-CTRL-Phase 1) and Institut Universitaire de France.

ORCID iD

Adrien Herledan <https://orcid.org/00000-0001-7258-498X>

Marine Andres <https://orcid.org/0000-0002-4943-7890>

Florence Leroux <https://orcid.org/0000-0003-0554-873X>

Biela Alexandre <https://orcid.org/0000-0001-5749-3262>

Catherine Piveteau <https://orcid.org/0000-0002-3835-4619>

Sandrine Warengem <https://orcid.org/0000-0001-9113-6058>

Cyril Couturier <https://orcid.org/0000-0002-6840-1738>

Benoit Deprez <https://orcid.org/0000-0002-2777-4538>

Rebecca Deprez-Poulain <https://orcid.org/0000-0002-3318-5297>

Supplementary Information is available online with this article

Design of the CETSA Protein Microarray patterns; Acquired images; Specificity of the anti-IDE antibody, ITDRF of 3 with IDE; Tagg of IDE; MS/MS parameters for 1-3; Supplementary Methods : LC-MS/MS analysis of CETSA samples, Solubility and Log D measurements, Docking ITDRF

Httpxxxxxxxxxxxxxxxxxxxxxxxxxxxx

Supplemental_Material_for_Tandem_CETSA_aRPPA_by_Herledan_et_al

References

1. Comess, K. M.; McLoughlin, S. M.; Oyer, J. A.; et al Emerging Approaches for the Identification of Protein Targets of Small Molecules - A Practitioners' Perspective. *J. Med. Chem.* **2018**, 61, 8504-8535
2. Lundgren, S. Focusing on Relevance: CETSA-Guided Medicinal Chemistry and Lead Generation. *ACS Med. Chem. Lett.* **2019**, 10, 690-693.

3. Shaw J, Dale I, Hemsley P *et al.* Positioning High-Throughput CETSA in Early Drug Discovery through Screening against B-Raf and PARP1. *SLAS Discov.* **2018**, 24(2), 121-132.
4. Jafari, R.; Almqvist, H.; Axelsson, H.; *et al.* The Cellular Thermal Shift Assay for Evaluating Drug Target Interactions in Cells. *Nat Protoc* **2014**, 9, 2100–2122.
5. Almqvist, H.; Axelsson, H.; Jafari, R.; *et al.* CETSA Screening Identifies Known and Novel Thymidylate Synthase Inhibitors and Slow Intracellular Activation of 5-Fluorouracil. *Nat Commun* **2016**, 7, 11040.
6. Savitski, M. M.; Reinhard, F. B. M.; Franken, H.; *et al.* Tracking Cancer Drugs in Living Cells by Thermal Profiling of the Proteome. *Science* **2014**, 346, 1255784.
7. Franken, H.; Mathieson, T.; Childs, D.; *et al.* Thermal Proteome Profiling for Unbiased Identification of Direct and Indirect Drug Targets Using Multiplexed Quantitative Mass Spectrometry. *Nat Protoc* **2015**, 10, 1567–1593.
8. Axelsson, H.; Almqvist, H.; Otrocka, M.; *et al.* *In Situ* Target Engagement Studies in Adherent Cells. *ACS Chem. Biol.* **2018**, 13, 942–950.
9. Massey, A. J. A High Content, High Throughput Cellular Thermal Stability Assay for Measuring Drug-Target Engagement in Living Cells. *PLoS ONE* **2018**, 13, e0195050.
10. Shaw, J.; Leveridge, M.; Norling, C.; *et al.* Determining Direct Binders of the Androgen Receptor Using a High-Throughput Cellular Thermal Shift Assay. *Sci. Rep.* **2018**, 8, 163-163.
11. McNulty, D. E.; Bonnette, W. G.; Qi, H.; *et al.* A High-Throughput Dose-Response Cellular Thermal Shift Assay for Rapid Screening of Drug Target Engagement in Living Cells, Exemplified Using SMYD3 and IDO1. *SLAS Discov.* **2017**, 23, 34-46.
12. Martinez, N. J.; Asawa, R. R.; Cyr, M. G.; *et al.* A Widely-Applicable High-Throughput Cellular Thermal Shift Assay (CETSA) Using Split Nano Luciferase. *Sci. Rep.* **2018**, 8, 9472.
13. Colin, B.; Deprez, B.; Couturier, C. High-Throughput DNA Plasmid Transfection Using Acoustic Droplet Ejection Technology. *SLAS Discov* **2019**, 24, 492-500.
14. Zhang, Z.; Liang, W. G.; Bailey, L. J.; *et al.* Ensemble cryoEM elucidates the mechanism of insulin capture and degradation by human insulin degrading enzyme. *eLife* **2018**, 7, e33572.

15. Charton, J.; Gauriot, M.; Guo, Q.; *et al.* Imidazole-derived 2-[N-carbamoylmethyl-alkylamino]acetic acids, substrate-dependent modulators of insulin-degrading enzyme in amyloid- β hydrolysis. *Eur.J. Med. Chem.* **2014**, 79, 184-193.
16. Charton, J.; Gauriot, M.; Totobenazara, J.; *et al.* Structure-activity relationships of Imidazole-derived 2-[N-carbamoylmethyl-alkylamino]acetic acids, dual binders of human Insulin-Degrading Enzyme. *Eur.J. Med. Chem.* **2015**, 90, 547-567.
17. Maianti, J. P.; McFedries, A.; Foda, Z. H.; *et al.* Anti-diabetic activity of insulin-degrading enzyme inhibitors mediated by multiple hormones. *Nature* **2014**, 511, 94-98.
18. Deprez-Poulain, R.; Hennuyer, N.; Bosc, D.; *et al.* Catalytic site inhibition of insulin-degrading enzyme by a small molecule induces glucose intolerance in mice. *Nature Comm.* **2015**, 6, 8250.
19. Villa-Perez, P.; Merino, B.; Fernandez-Diaz, C. M.; *et al.* Liver-specific ablation of insulin-degrading enzyme causes hepatic insulin resistance and glucose intolerance, without affecting insulin clearance in mice. *Metabolism* **2018**, 88, 1-11.
20. Wong, E. Y.; Diamond, S. L. Advancing Microarray Assembly with Acoustic Dispensing Technology. *Anal. Chem.* **2009**, 81, 509–514.

Figures Legends

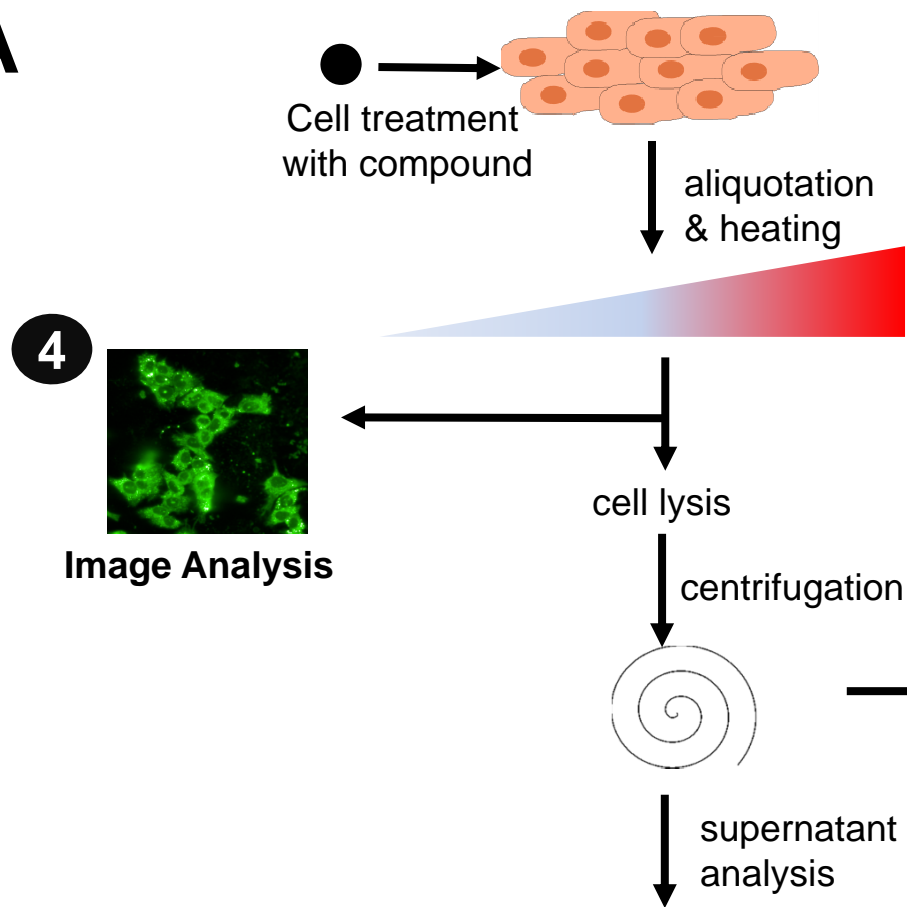
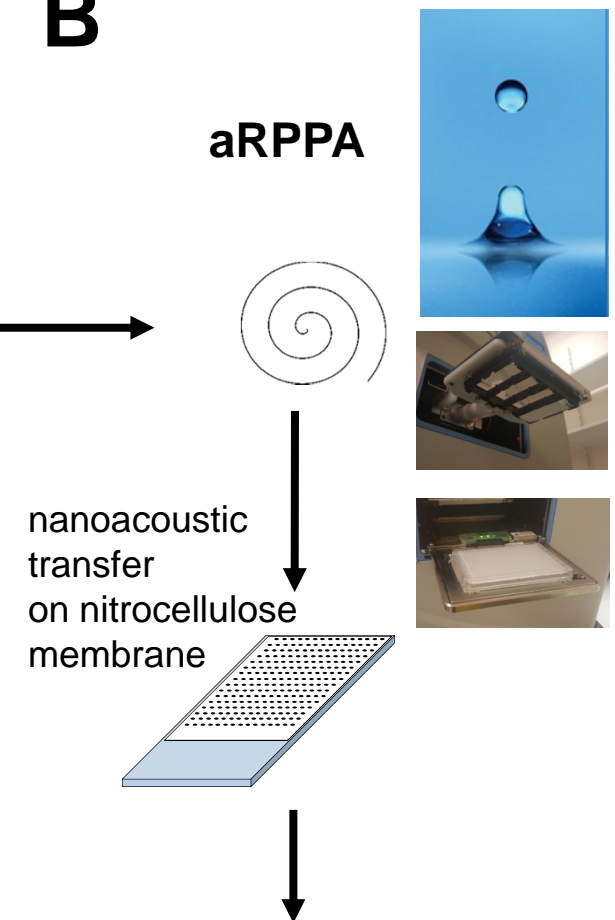
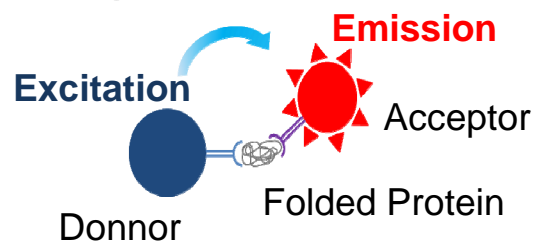
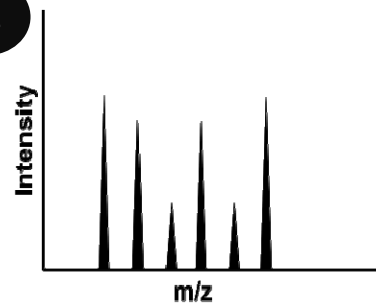
Figure 1. Current protocols of CETSA and proposed CETSA-aRPPA. **(A)** Current protocols and formats for CETSA: Classic (1), High-throughput (2), Mass-spectrometry (3) and imaging (4). **(B)** Proposed CETSA-aRPPA format using nano acoustic dispensing and protein array immunoblotting.

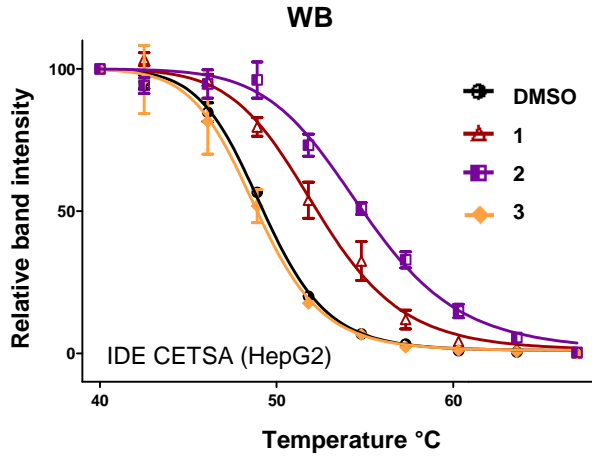
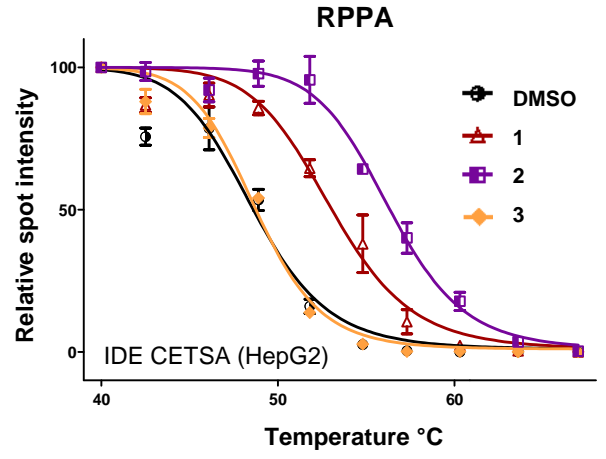
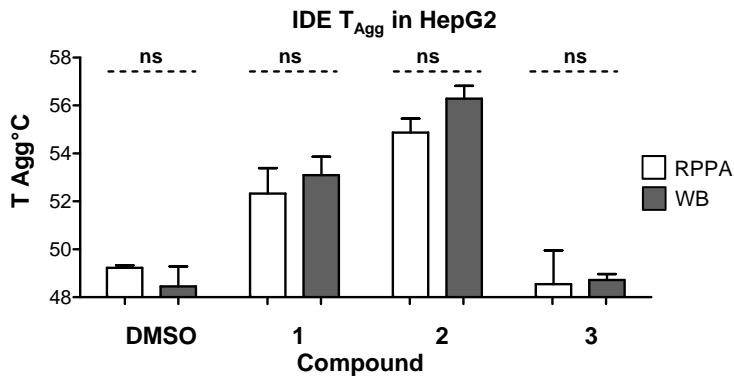
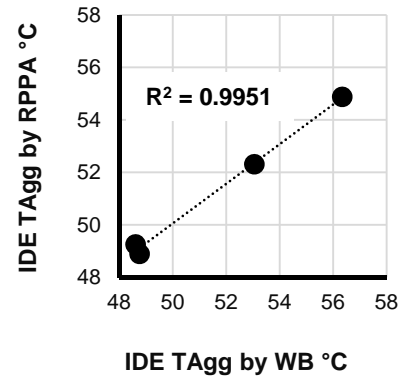
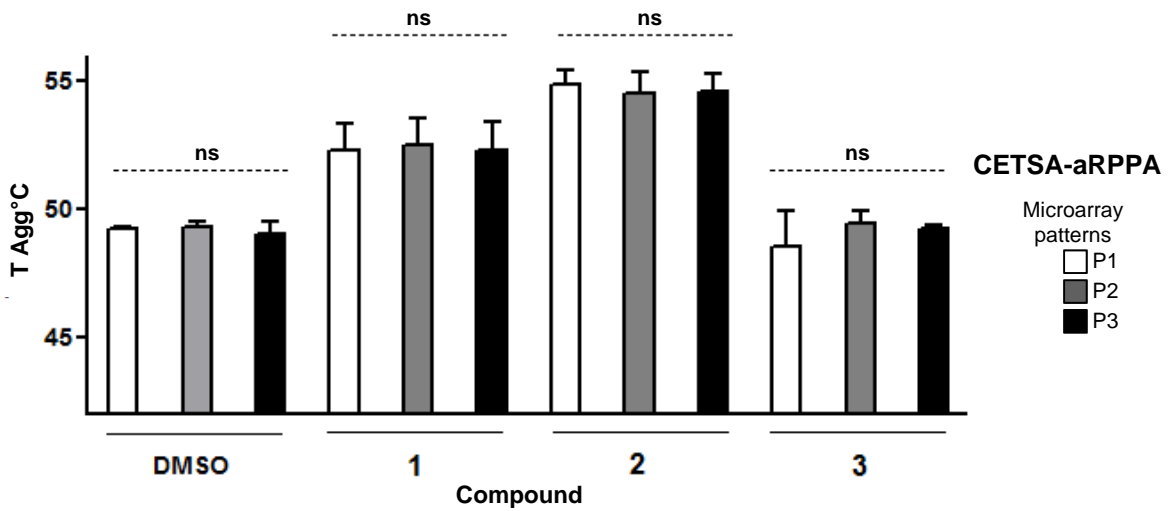
Figure 2. Validation of CETSA-aRPPA assay to screen for intracellular target engagement, in comparison with classical CETSA-WB, in HepG2 cells. HepG2 cells were treated for 2 h with DMSO vehicle or compounds (30 μ M) before applying heatshock, lysis, and quantification by aRPPA or WB. Aggregation curves of IDE in the absence and presence of inhibitors determined by Western Blot **(A)** and by RPPA **(B)** and aggregation temperature (T_{Agg}) **(C)** determined using chemical denaturation theory formula. WB in gray bars, RPPA in open bars, for vehicle (DMSO) and compounds **1-3**. **(D)** Correlation of IDE T_{Agg} measured by the 2 techniques with or without compound, showing that aRPPA is as accurate as WB. **(E)** Precision of aRPPA for IDE aggregation temperature (T_{Agg}) measurement, evaluated in the absence or presence of compounds mean of three aRPPA patterns (P1, P2, P3) each done in triplicate. Data presented in panels **A** to **E** are from the same experiment. Statistic were performed using one way ANOVA ($p < 0.001$, followed by Tukey's test, $n = 3$), ns : non significant

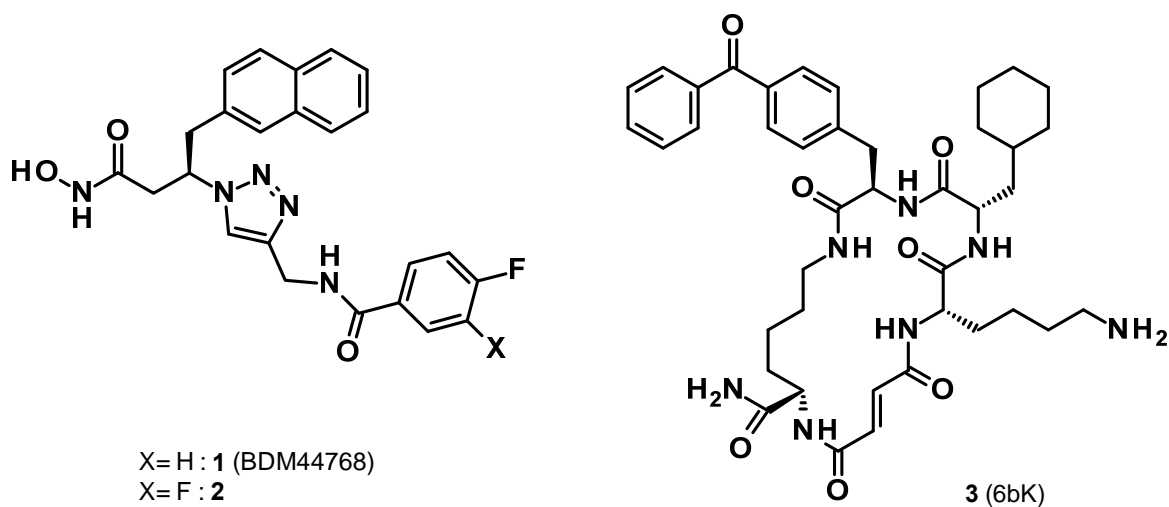
Figure 3. Evaluation of thermal stabilization of IDE in HepG2 cells by inhibitors **1-3**. **(A)** Structures of inhibitors **1-3**. **(B)** Properties and structural features of **1** (BDM44768), **2** (analog of BDM44768) and **3** (6bK). pIC_{50} on IDE using insulin as a substrate (mean of at least 3 experiments); **(C)** ΔT_{Agg} measured by aRPPA (from data in Fig. 2B). Values presented are the mean of ratios with \pm SD of the 3 independent CETSA experiments.

Statistics were performed using one way ANOVA ($p < 0.001$, followed by Tukey's test, $n = 3$). ΔT_{Agg} for **1** and **2** are displayed in dark red and purple respectively. Unlike compound **3**, **1** and **2** engage IDE in HepG2 cells as demonstrated by CETSA shifting IDE melting curves at 30 μM (Figure 2) compared with vehicle (DMSO), with a ΔT_{Agg} of respectively 3.1 $^{\circ}\text{C}$ and 5.6 $^{\circ}\text{C}$.

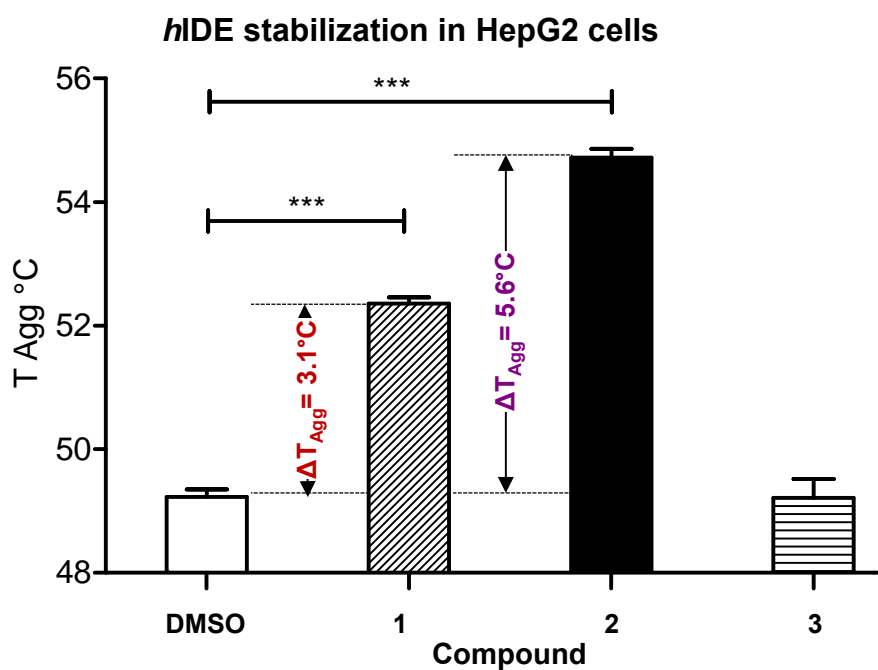
Figure 4. Dose-dependent stabilization (ITDRF_{CETSA-aRPPA}) of IDE in HepG2 cells by inhibitors **1-2**, and correlation with physchem properties. In-cell engagement of IDE by compound **1** (A) and **2** (B) determined by ITDRF, based on raw data from CETSA-aRPPA readings ($n = 3$) at 50.5 $^{\circ}\text{C}$, in the presence of increasing concentrations of compounds. **1** and **2** stabilize IDE in a dose-dependent manner. Samples were simultaneously probed for anti-IDE and anti-tubulin (loading control). (C) Permeability as the ratio of compound concentrations (LC-MS/MS analysis) respectively in HepG2 cells and medium samples in CETSA experiments after 2 h of incubation. Values presented are the mean of ratios with \pm SD of the 3 independent CETSA experiments. Statistics were performed using one way ANOVA ($p < 0.001$, followed by Tukey's test, $n = 3$). (D) Potency of compounds pIC_{50} , target engagement EC_{50} , permeability as the ratio of cell/medium concentration, cellular potency shift as the ratio of EC_{50} target engagement / IC_{50} on IDE; aqueous solubility and LogD for compounds **1** and **2**. Introduction of second fluorine in compound **2** enhances IDE inhibition, LogD and cell permeability while decreasing aqueous solubility in comparison with **1**. (E) Docking of compound **2** in IDE structure (PDB: 4NXO). Compound **2**: C (orange), O (red), N (blue); F (light blue); zinc (magenta sphere); N-terminal domain residues, (green) C-terminal domain residues (purple); electrostatic, π - π interaction, and hydrogen bonds in dotted lines.

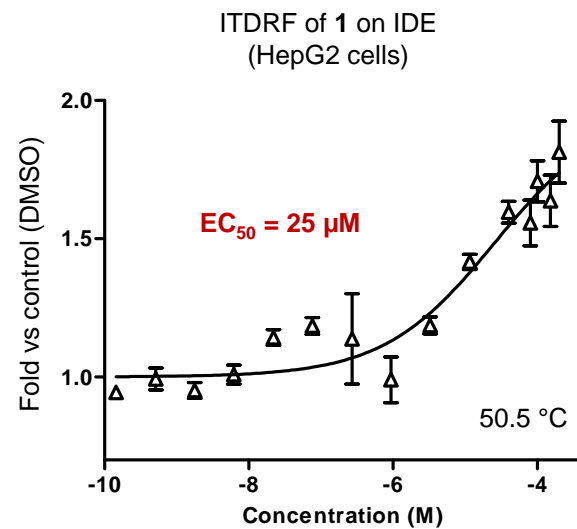
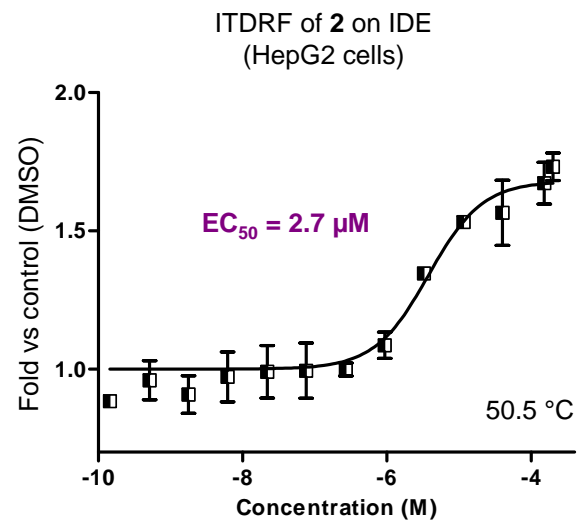
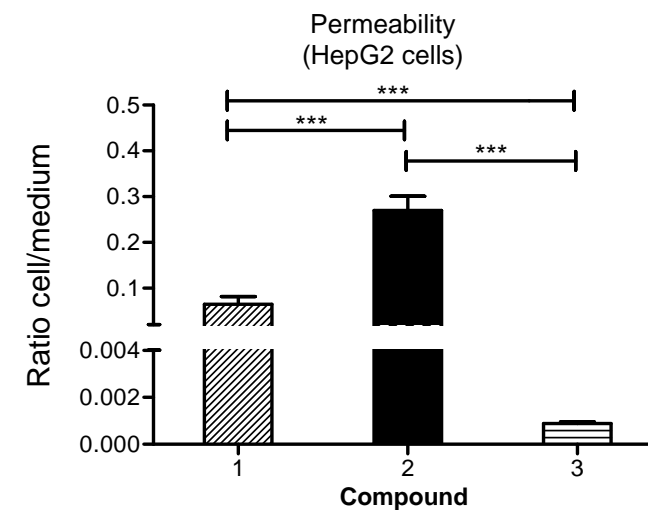
A**B****1****Western Blot****2****Homogeneous Detection
(AlphaScreen®-based assay)****3****High-Resolution
Mass Spectrometry****5****Protein Array
Immunoblotting**

A**B****C****D****E**

A**B**

Cpd ▶	1 (BDM44768)	2	3 (6bK)
hIDE pIC ₅₀	6.48	6.89	6.77
MW (g/mol)	447.46	465.45	757.92
# Heavy atoms	33	34	55
Ligand efficiency	0.31	0.28	0.17
Structural type	small molecule	small molecule	macrocycle
Binding site	Catalytic site	Catalytic site	Exosite

C

A**B****C****D**

Cpd ▶	1	2
hIDE pIC ₅₀	6.48	6.89
Target engagement (ITDRF) EC ₅₀ (μM)	25 ± 13	2.7 ± 1.9
Cellular potency shift (EC ₅₀ /IC ₅₀)	77	21
Permeability (cell/medium ratio)	0.065 ± 0.016	0.27 ± 0.03
Aqueous solubility (μM)	56	11
LogD	2.2	2.6

E